STEELS

Literature:

1. M. Blicharski, Stal', WN-T, Warszawa 2004,
2. M.F. Aschby, D.R.H. Jones, Materiały inżynierskie. Cz.2 Warszawa 1996.
3. L. Dobrzański Metalowe materiały inżynierskie, Wyd. Naukowo Techniczne, Warszawa 2004
4 J. Adamczyk, Inżynieria wyrobów stalowych, Wyd. Politechniki Śląskiej, Gliwice, 2000

According to Worldsteel.org w 2006 in the world was produced 1 244 milions

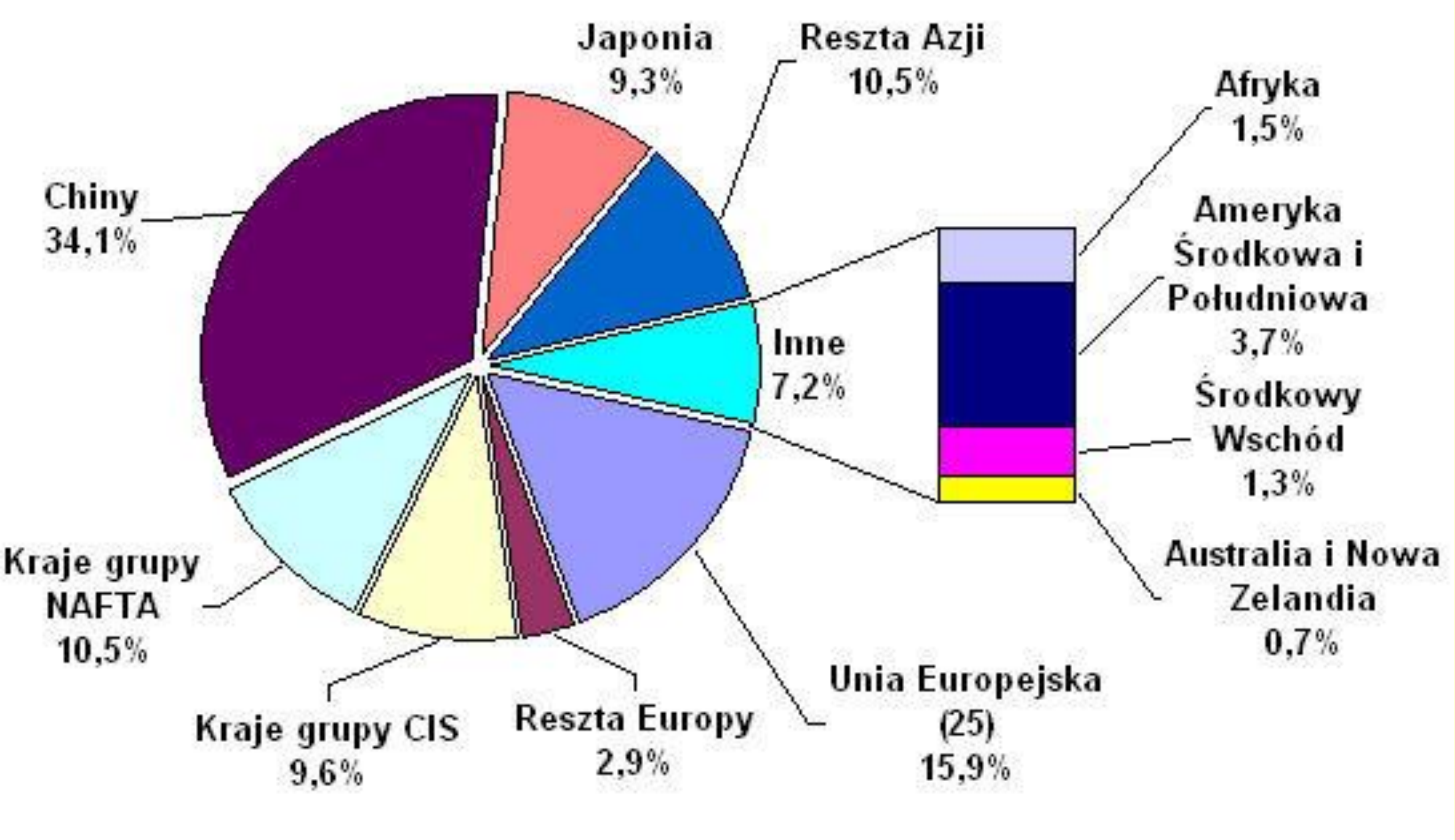

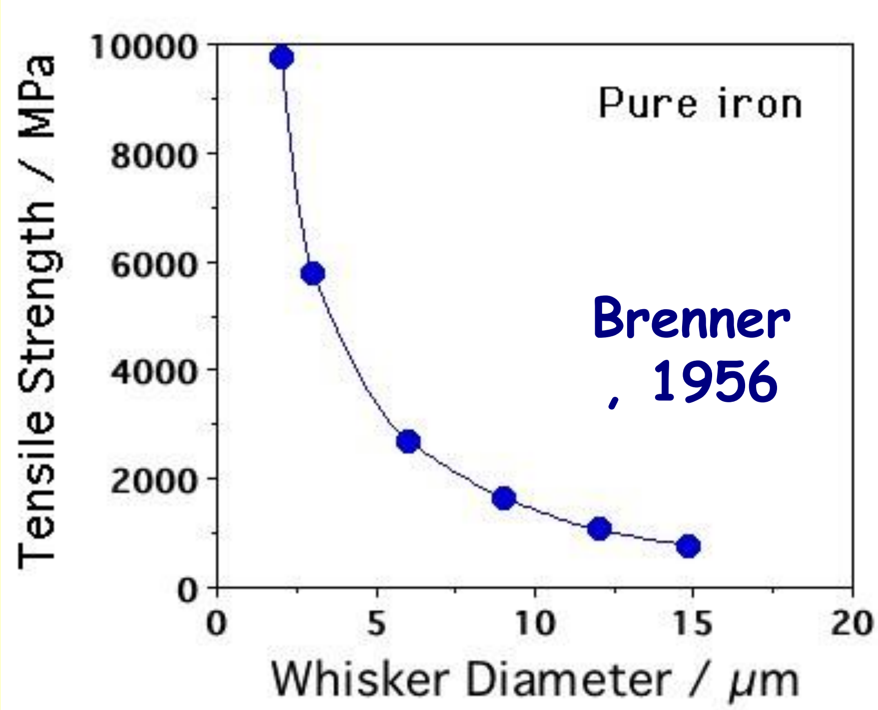

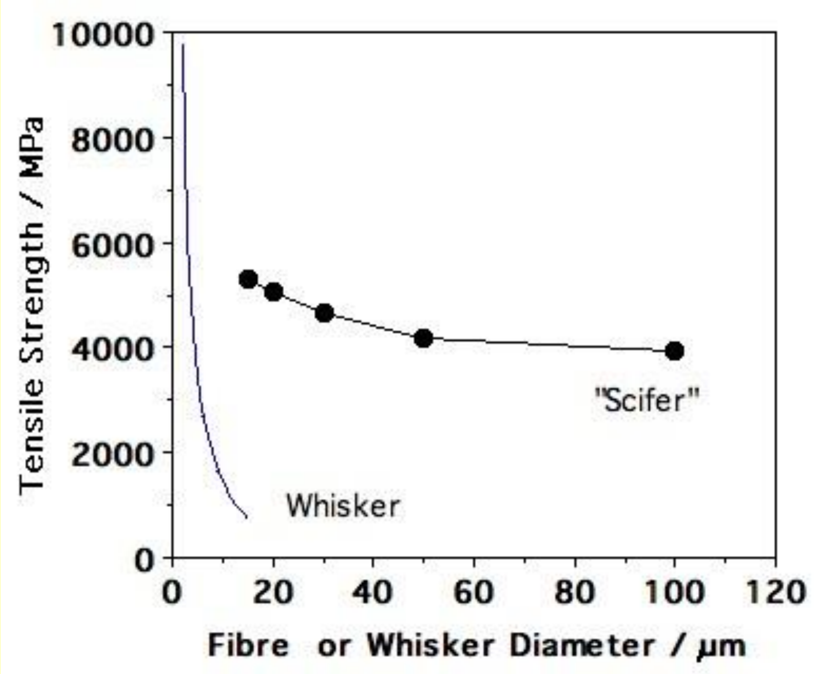

Kobe Steel

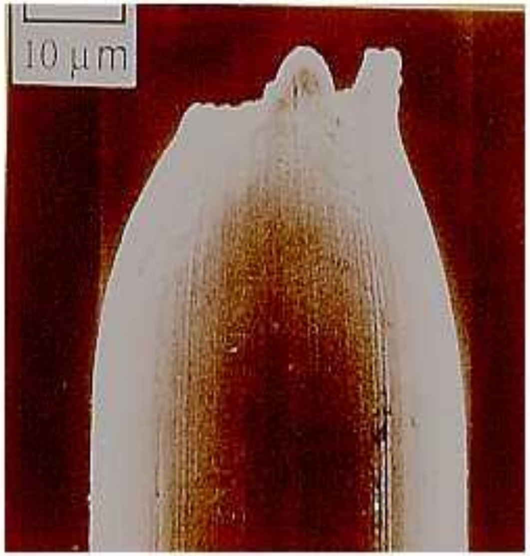

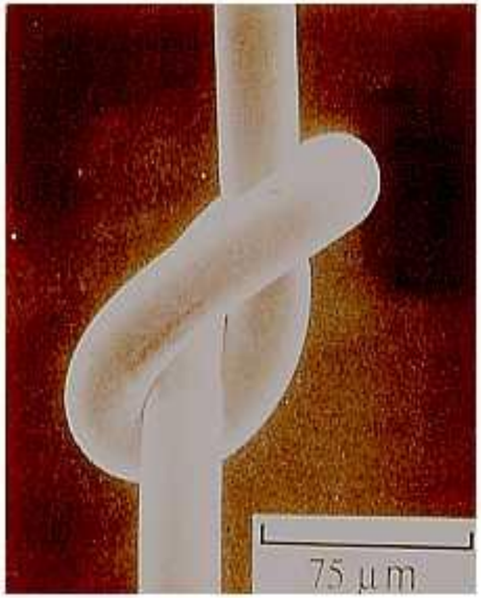

Scifer, 5.5 GPa and ductile

RECONSTRUCTIVE

Diffusion of all atoms during nucleation and growth.
Sluggish below about 850 K.

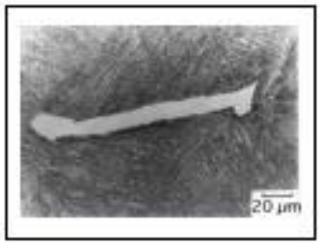

ALLOTRIOMORPHIC FERRITE

IDIOMORPHIC FERRITE

MASSIVE FERRITE

No change in bulk composition.

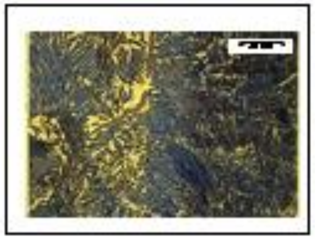

PEARLITE

Cooperative growth of ferrite & cementite.

DISPLACIVE

Invariant-plane strain shape deformation with large shear component.
No iron or substitutional solute diffusion.
Thin plate shape.

Ferryt iglasty (Blicharski)

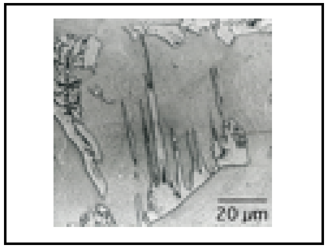

WIDMANSTÄTTEN FERRITE

Carbon diffusion during paraequilibrium nucleation & growth.

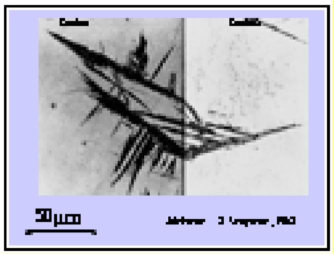

BAINITE & ACICULAR FERRITE

Carbon diffusion during paraequilibrium nucleation. No diffusion during growth.

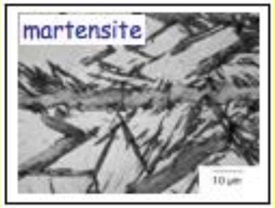

MARTENSITE

Diffusionless nucleation & growth.

Allotriomorphic Ferrite

An allotriomorph has a shape which does not reflect its internal crystalline symmetry. This is because it tends to nucleate at the austenite grain surfaces, forming layers which follow the grain boundary contours (Fig. 1).

An idiomorph on the other hand, has a shape which reflects the symmetry of the crystal as embedded in the austenite. Idiomorphs nucleate without contact with the austenite grain surfaces; they tend to nucleate heterogeneously on non–metallic inclusions present in the steel.

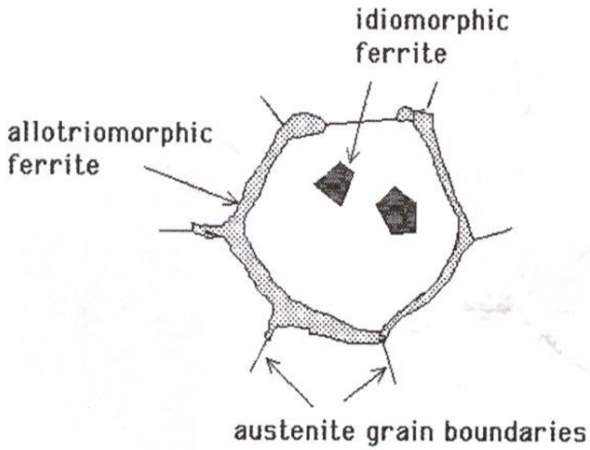

Fig. 1: Allotriomorphic & idiomorphic ferrite.

These are both true diffusional transformations, *i.e.,* there is no atomic correspondence between the parent and product crystals, there is no invariant–plane strain shape change accompanying transformation, the growth rate is either diffusion–controlled, interface–controlled or mixed. Thermal activation is necessary for transformation, which can therefore only occur at high homologous temperatures.

Carbon steels Fe-C phase diagram Fe-Fe_3C

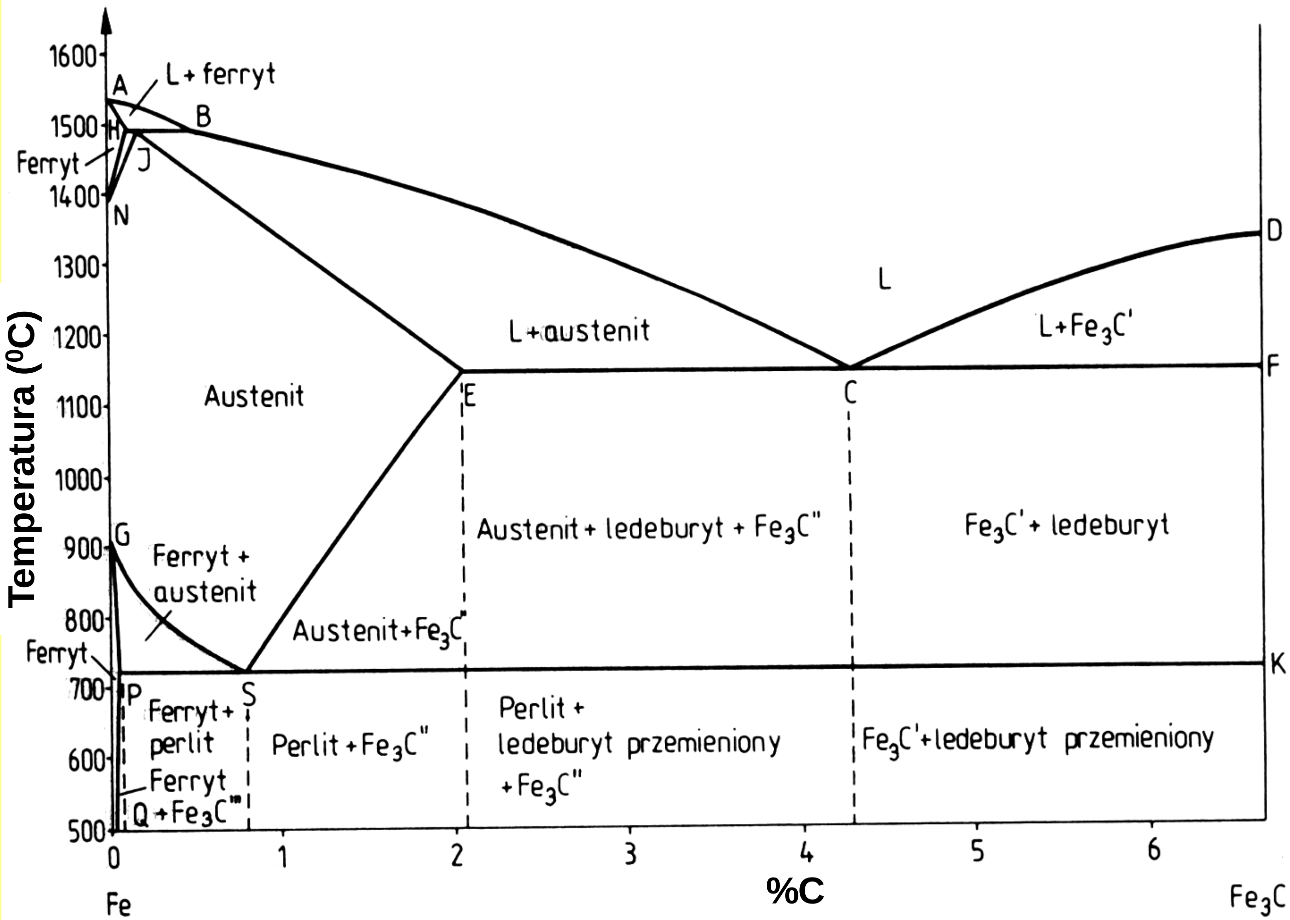

Ozn.	A	B	C	D	E	G	H	J	N	P	S	Q
%C	0	0,53	4,30	6,67	2,11	0	0,09	0,17	0	0,0218	0,77	0,008
Temp.,°C	1538	1495	1148	1227	1148	912	1495	1495	1394	727	727	20

Mechanical properties of steels in normalized state

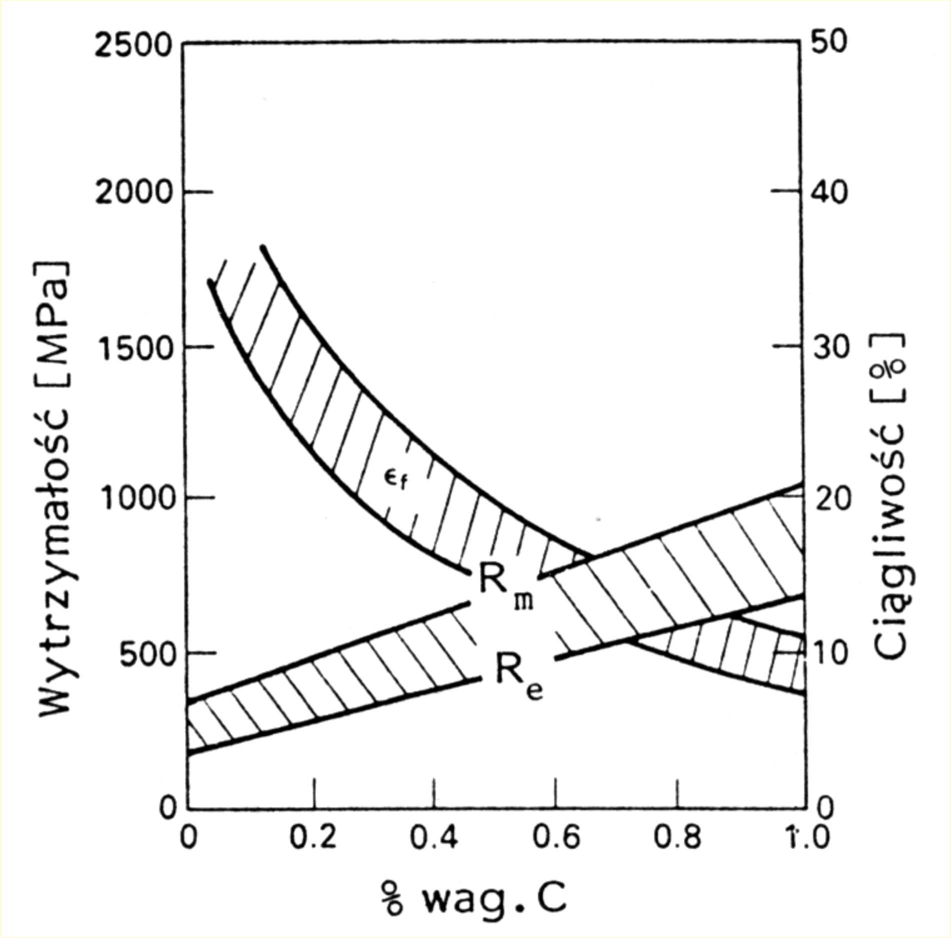

R_e i R_m – grow linearly with carbon contentC,

Plasticity decreases rapidly with carbon content–

Heat treatment of carbon steels

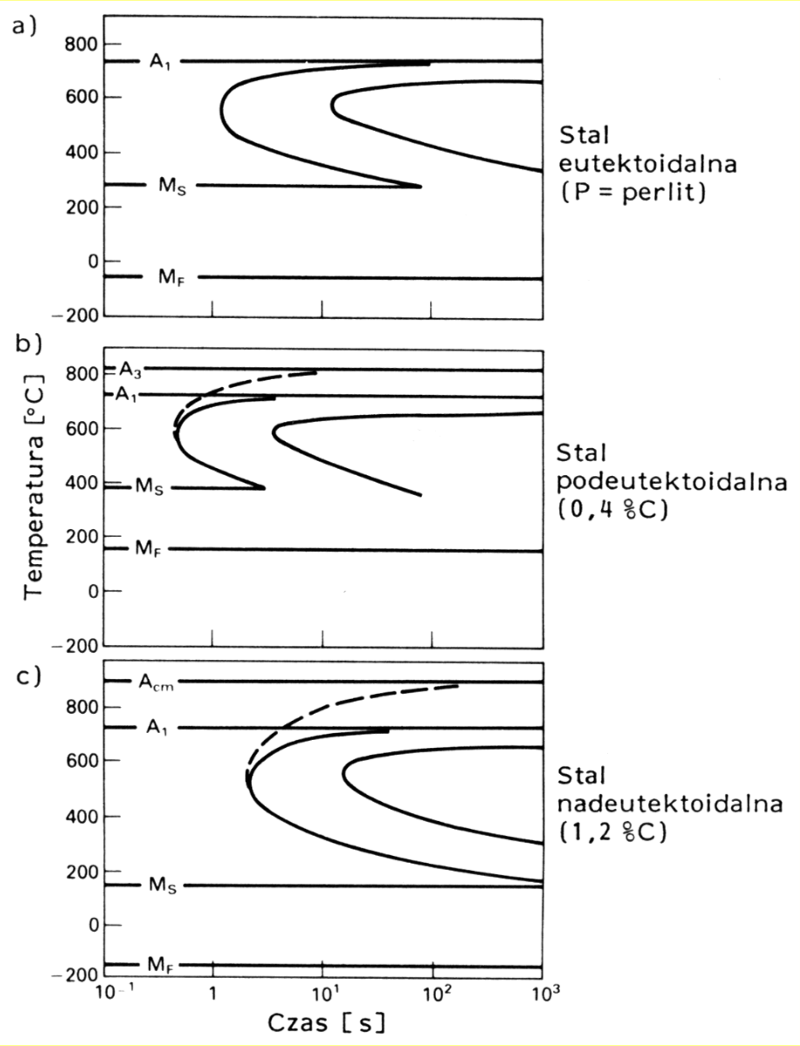

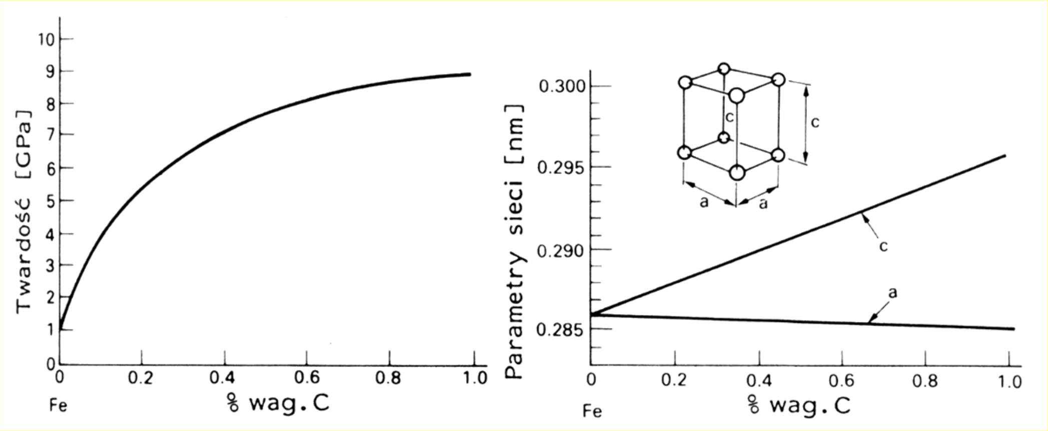

Hardness of martensite groews due to growth of stresses.

CTP curves for carbon steels: (a) eutektoid, (b) subdeutektoidalnej, (c) hipereutektoid. When carbon content grows, the M_s and M_f. drop

Constructional nonalloyed steels

Skład chemiczny i własności mechaniczne niestopowych stali konstrukcyjnych i maszynowych

Znak stali [1]	Maksymalne stężenie pierwiastków [2], %						Minimalne własności mechaniczne					
	C	Mn	Si	P	S	N	R_m [3], MPa	R_e [4], MPa	A_{80mm} [5], %	A [6], %	Temp. próby, °C	KV [7]
S185	–	–	–	–	–	–	290	185	14	18	–	–
S235JR S235JRG1 S235JRG2 S235J0 S235J2G3 S235J2G4	0,2 0,2 0,17 0,17 0,17 0,17	1,4	–	0,045 0,045 0,045 0,04 0,035 0,035	0,045 0,045 0,045 0,04 0,035 0,035	0,009 0,007 0,009 0,009 – –	340	235	21	26	20 20 20 0 -20 -20	27
S235JRG2C [8]	0,17	1,4	–	0,045	0,045	0,009	420	300	–	9	–	–
S275JR S275J0 S275J2G3 S275J2G4	0,21 0,18 0,18 0,18	1,5	–	0,045 0,04 0,035 0,035	0,045 0,04 0,035 0,035	0,009 0,009 – –	410	275	18	22	20 0 -20 -20	27
S355JR S355J0 S355J2G3 S355J2G4 S355K2G3 S355K2G4	0,24 0,2 0,2 0,2 0,2 0,2	1,6	0,55	0,045 0,04 0,035 0,035 0,035 0,035	0,045 0,04 0,035 0,035 0,035 0,035	0,009 0,009 – – – –	490	355	18	22	20 0 -20 -20 -20 -20	27 27 27 27 40 40
S355J2G3C [8]	0,2	1,6	0,55	0,035	0,035	–	600	450	–	7	–	–
C10 [8] C15 [8] C16 [8]	0,13 0,18 0,18	0,6 0,8 0,9	0,4	0,045	0,045	–	430 480 500	300 340 360	–	9 8 8	–	–
E295 E335 E360 E295GC [8] E335GC [8]	–	–	–	0,045	0,045	0,009	470 570 670 600 680	295 335 360 420 480	16 12 8 – –	20 16 11 7 6	–	–

[1] Bez dodatkowego symbolu oraz JR - stale podstawowe; J0, J2 i K2 - stale jakościowe (porównaj przypis na str. 163).
[2] Skład chemiczny według analizy wytopowej produktów hutniczych o grubości od 16 do 40 mm (zgodnie z PN-EN 10025:2002); ograniczenie stężenia N nie obowiązuje jeśli Al ≥0,02% lub jest wystarczające stężenie innych pierwiastków wiążących azot. [3)÷7)] Próbki wzdłużne z produktów o grubości (w mm): [3] 2,5÷3, [4] 3÷100, [5] <16, [6] 3÷40, [7] 10÷150.
[4] W zależności od gatunku stali R_{eH} lub $R_{p0,2}$. [8] Stale według PN-EN 10277-2:2002; własności produktów o grubości 10÷16 mm w stanie ciągnionym na zimno (+C).

The effect of alloying additions on the pahse composition in steels

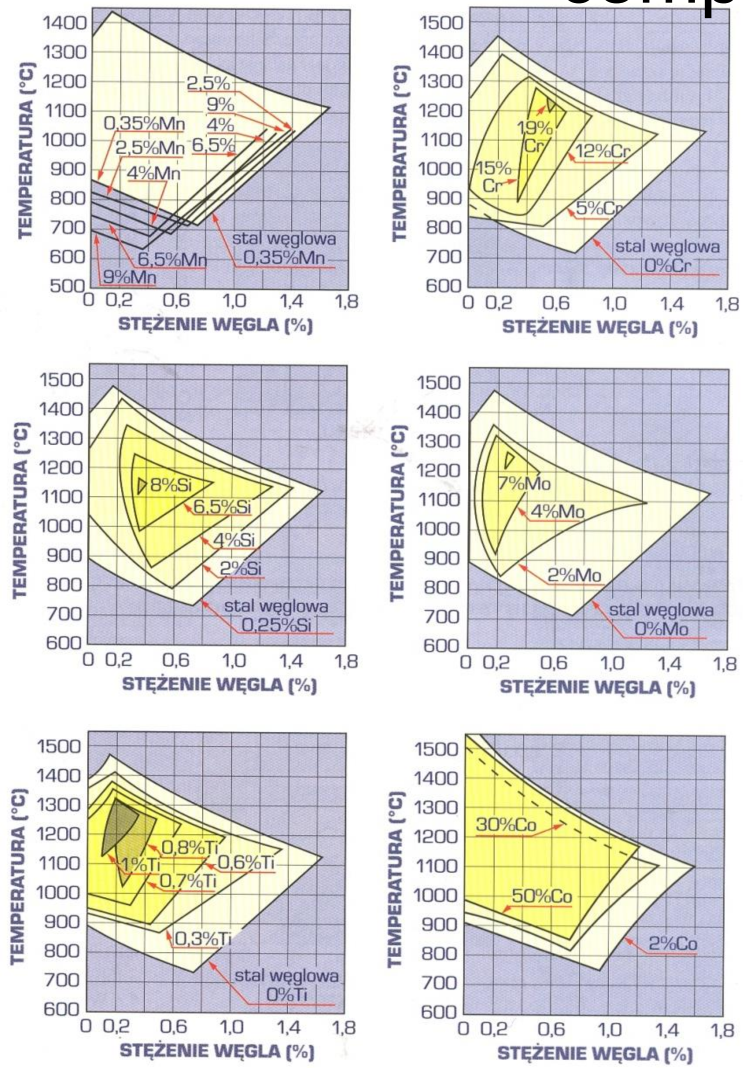

których pierwiastków stopowych oraz temperatury na zakres występowania austenitu węglem i danym pierwiastkiem (według E.C. Baina)

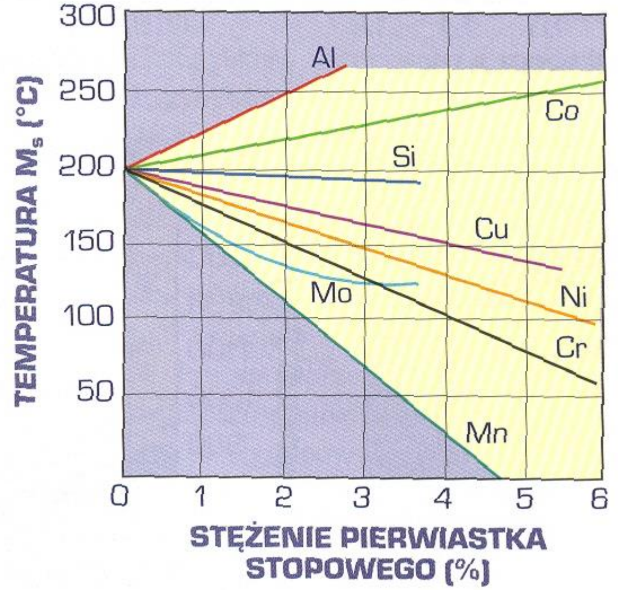

Rysunek 3.17

Wpływ stężenia składników stopowych na temperaturę początku przemiany martenzytycznej M_s w stali zawierającej ok. 1% C (według A.P. Gulajewa)

TRIP steels (Transformation Induced Plasticity)

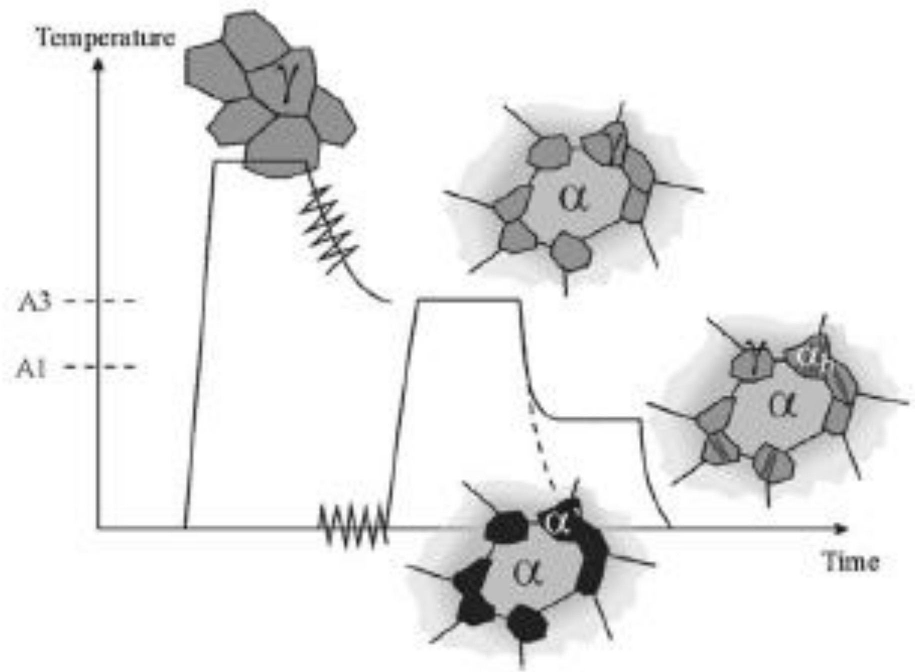

Fig. 2. Schematic representation of the thermomechanical treatments applied to hot or cold rolled TRIP-assisted multiphase steels (γ: austenite, α: ferrite, α': martensite, α_b: bainite).

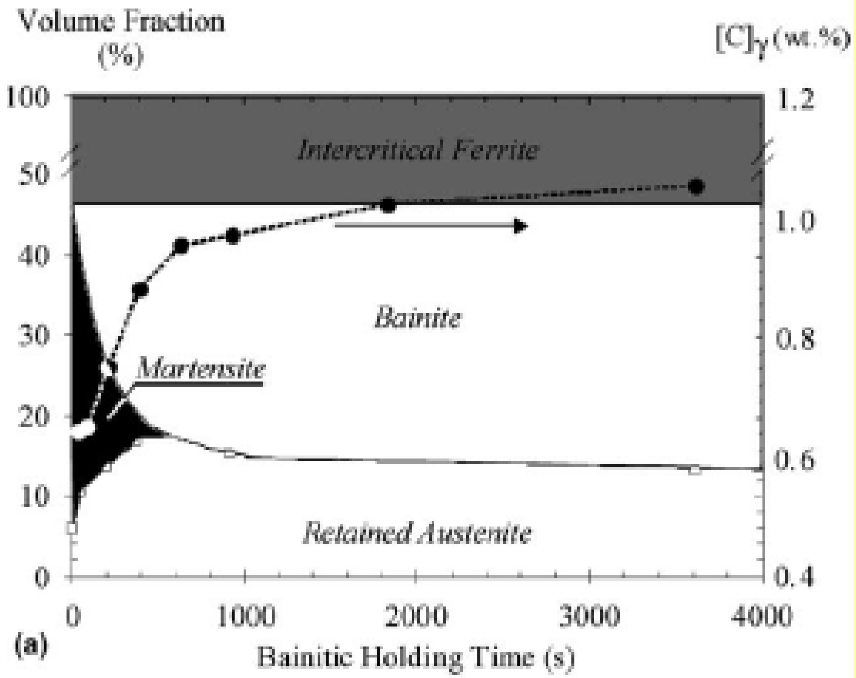

TRIP steels

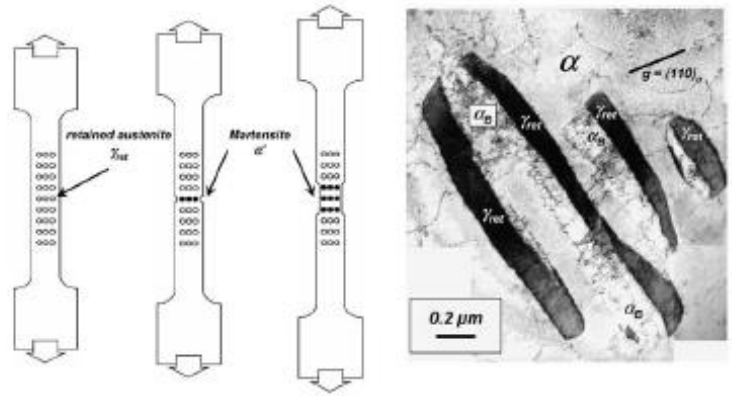

Fig. 10. Schematic of the TRIP-aided plasticity mechanism in low alloy TRIP steels. During straining the retained austenite transforms to martensite. The austenite is replaced by a high strength high C martensite, and the transformation is associated with a volume expansion. Both effect suppress plastic instability and extend the range of uniform elongation. The retained austenite, which is closely associated with the bainite, is present as small austenite islands, the diameter of which is typically in the range of 0.1–1.0 µm. Note that the retained austenite has an elongated shape.

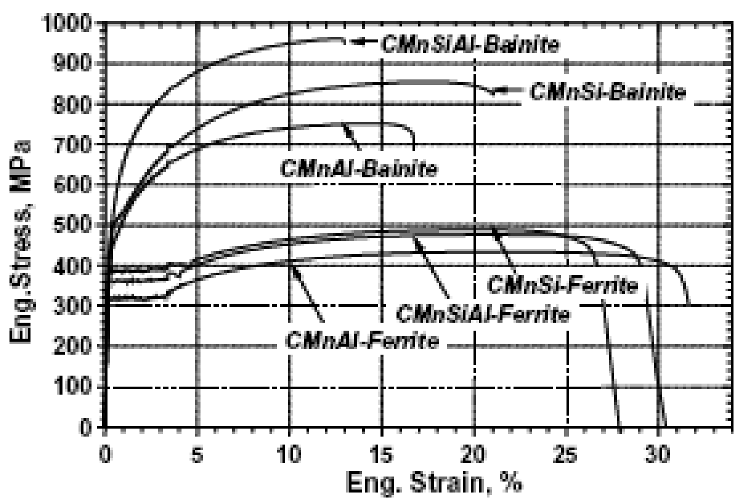

Fig. 17. Stress–strain curves for the isolated ferrite and bainite phase, both which are normally present as matrix and dispersed phase in low alloy TRIP steel, respectively. Note the relatively large Lüders strain associated with the ferrite. The bainite is associated with the absence or a very limited Lüders strain, a pronounced work-hardening and a very low yield-to-tensile strength ratio.

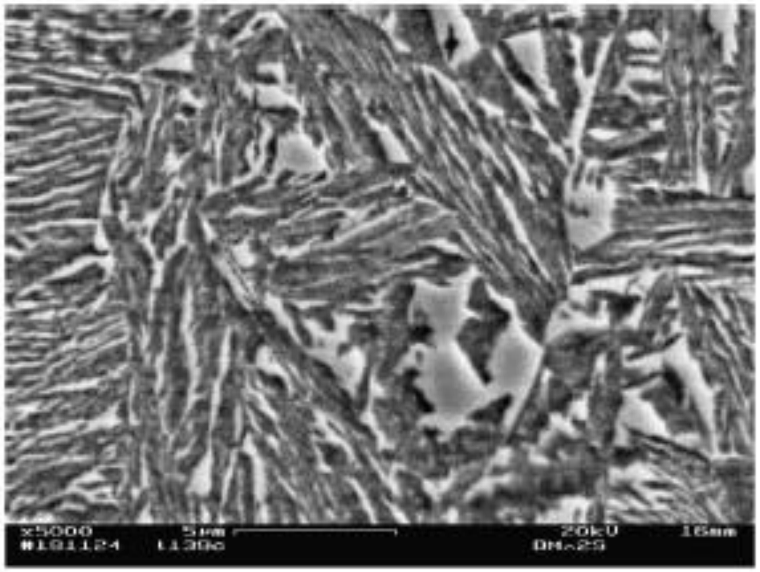

Fig. 16. SEM micrograph of the bulk CMnSiAl bainite phase (0.39 wt.% C, 1.72 wt.% Mn, 0.53 wt.% Si, 1.02 wt.%, Al, 0.011 wt.% P), which contains ~15 vol% retained austenite with 1.9 wt.% C. The retained austenite is present both as film between bainite laths and as a larger blocky phase.

TRIP steels

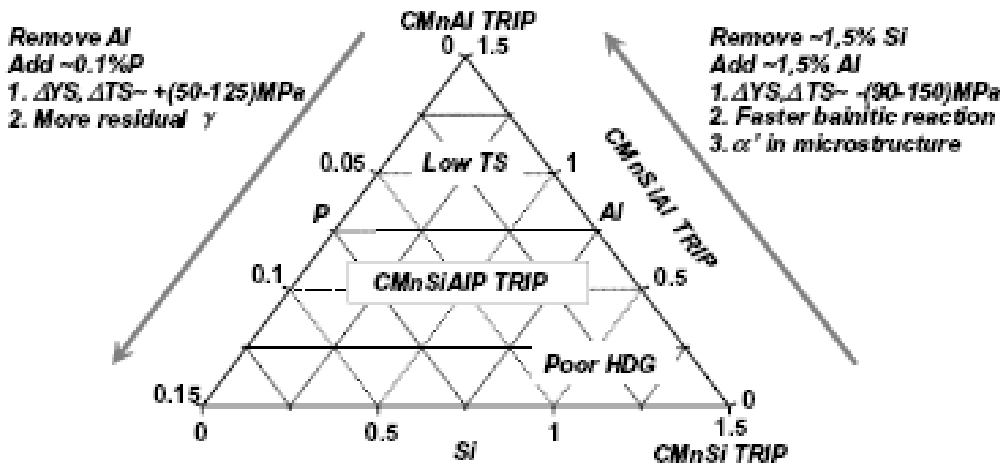

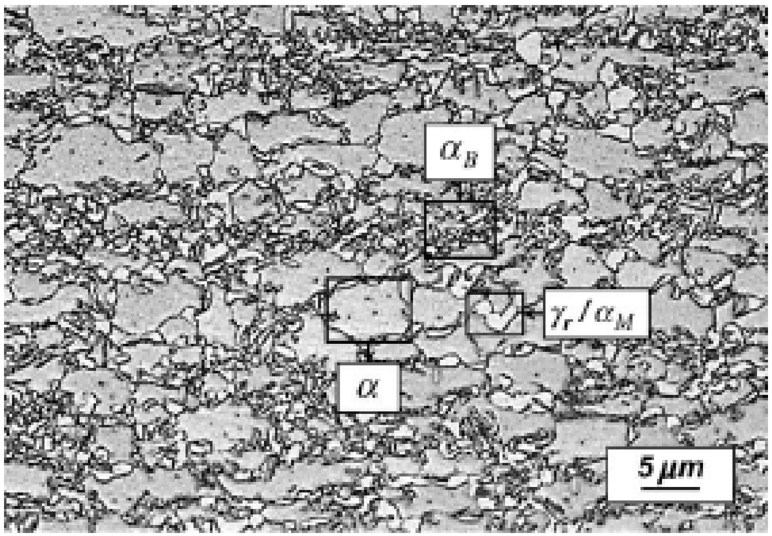

Fig. 6. Light optical micrographs of a color-etched TRIP steel micro-structure showing a clear difference between the micro-structural constituents (Micrograph courtesy of Dr. A.K. De, Colorado School of Mines).

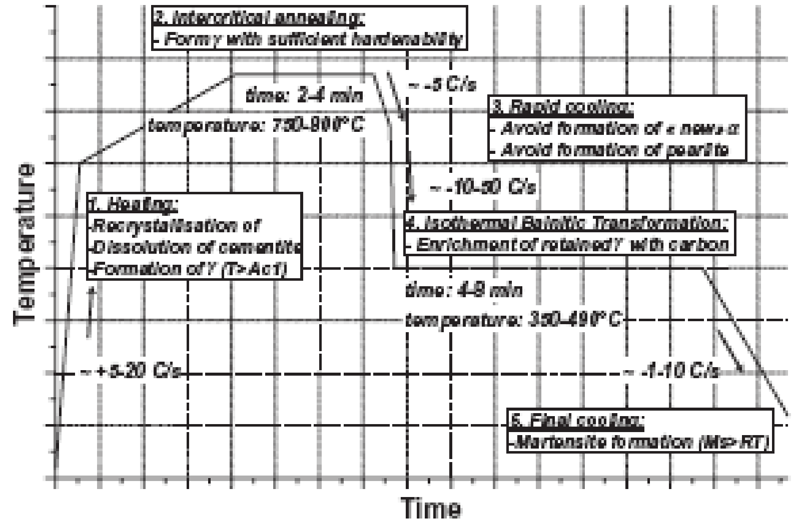

Fig. 7. Schematic of the intercritical processing for cold rolled low alloy TRIP steel: the main features of the five processing stages are indicated.

Ultra-low carbon bainitic steels – ULCB

Nr	C	Si	Mn	Ni	Mo	Cr	Nb	Ti	B	Al	N
8	0,020	0,20	2,00	0,30	0,30	-	0,050	0,020	0,0010	-	0,0025
9	0,028	0,25	1,75	0,20	-	0,30	0,100	0,015	-	0,030	0,0035

Carbon content limited to 0,01-0,03%C

Steels ULCB very good combination of strength and ductitlity,.

Cementite suppressed using silicon

1 μm

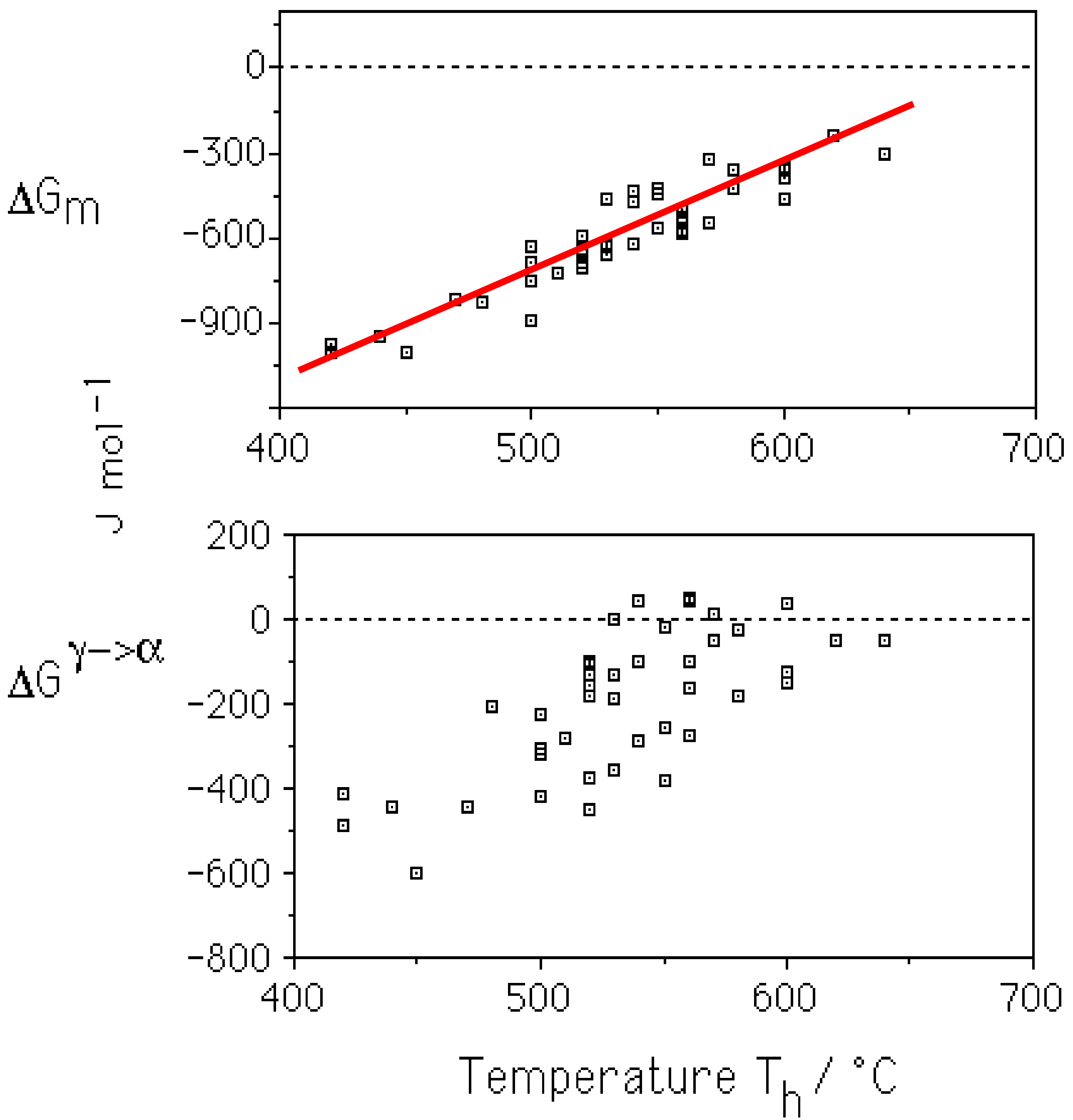

Each point represents a different steel

Nucleation function G_N

Bhadeshia, 1981

The nucleation of bainite must involve the partitioning of carbon

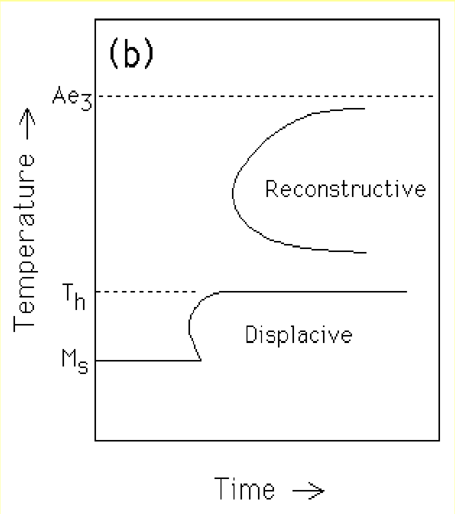

Why does the required free energy vary linearly with T?

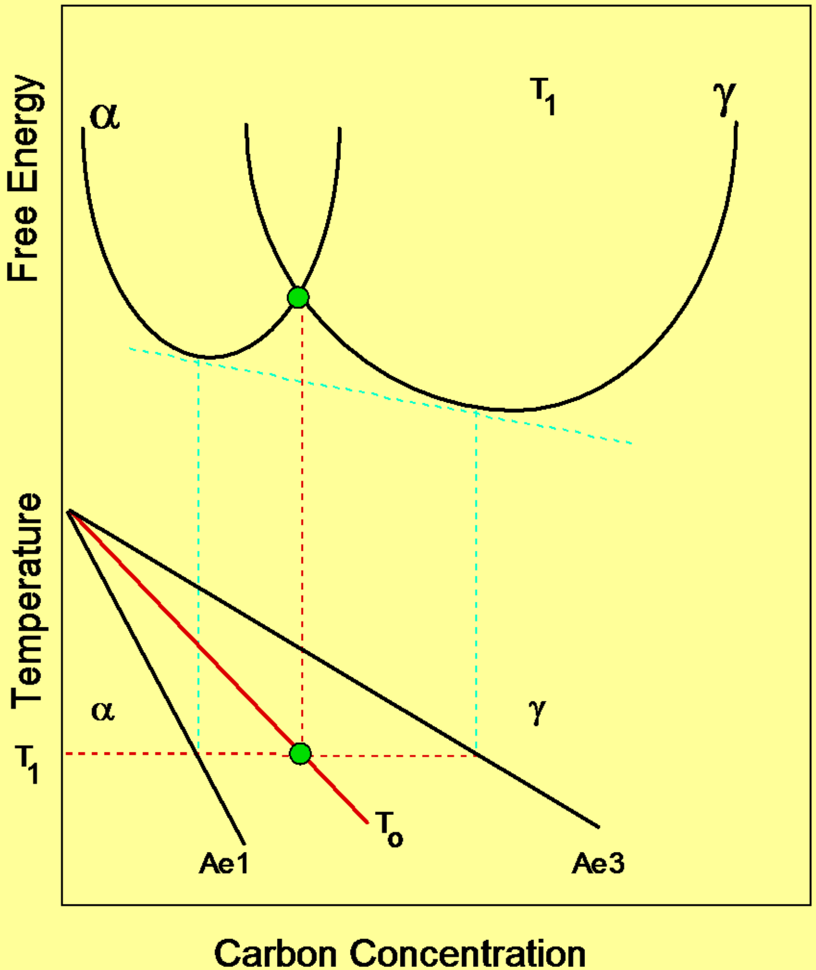

$$I \propto \nu \exp\{-G^*/RT\}$$

$$-G^* \propto \beta T \qquad \beta = R \ln\{I/\nu\}$$

$$\therefore G_N \propto \beta T_h$$

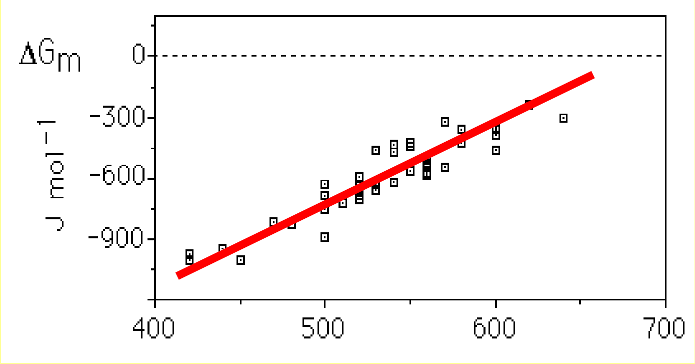

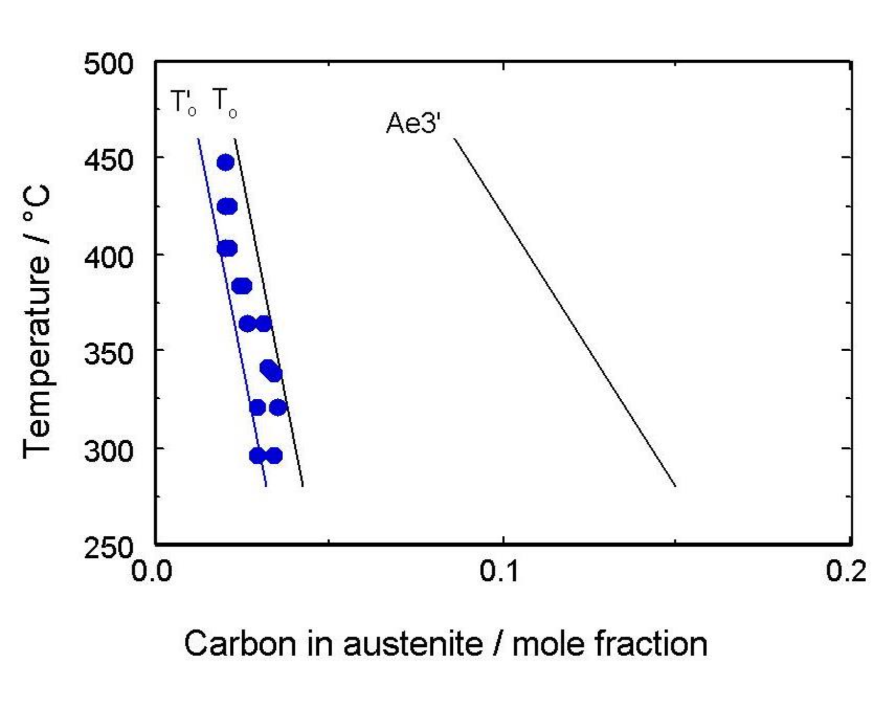
T'o
To
Ae3'
500
450
400
350
300
250
0.0
0.1
0.2
Temperature / °C
Carbon in austenite / mole fraction

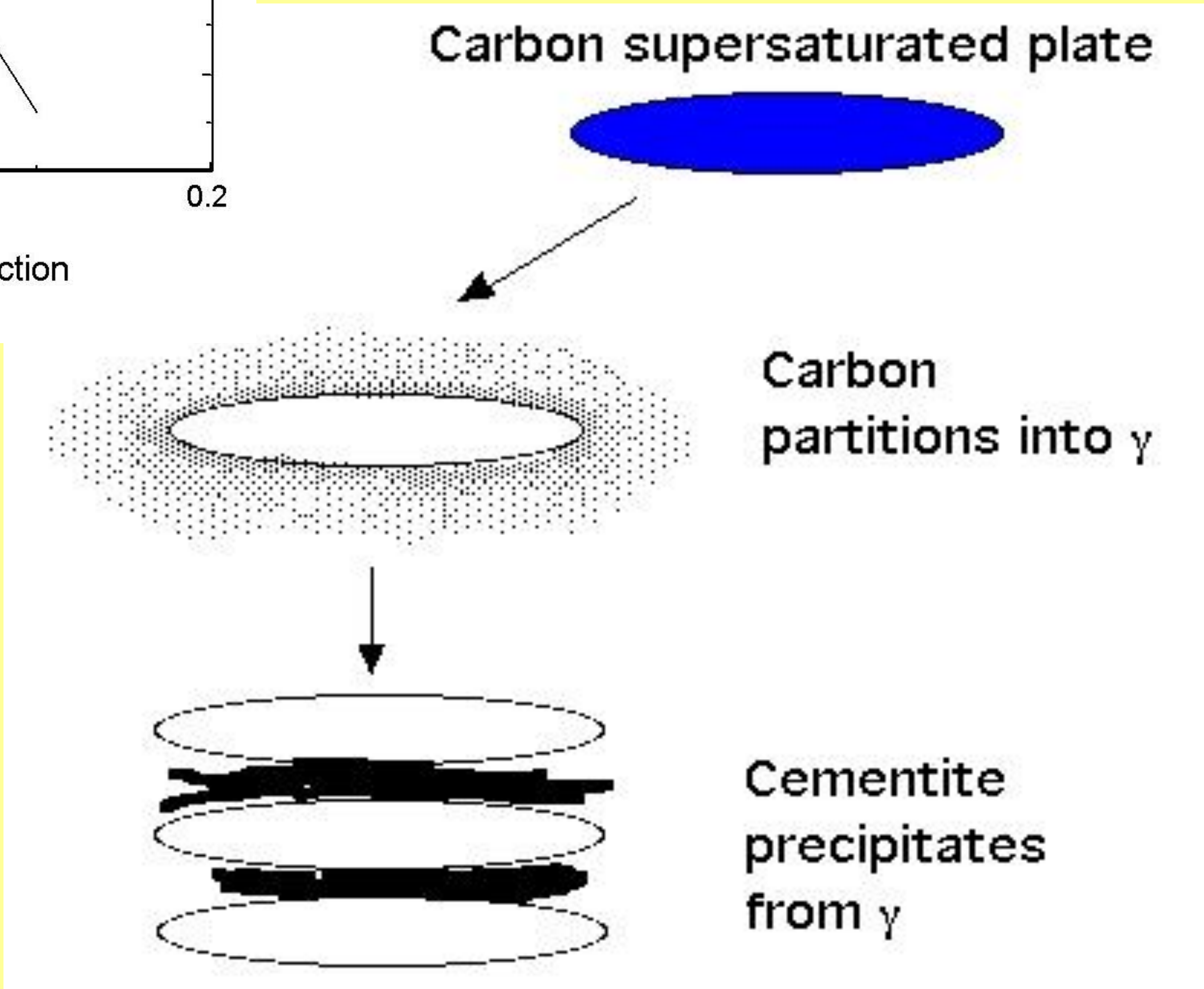
Carbon supersaturated plate
Carbon partitions into γ
Cementite precipitates from γ

Fe-2Si-3Mn-C wt%

C	Si	Mn	Mo	Cr	V	P
0.98	1.46	1.89	0.26	1.26	0.09	< 0.002

wt%

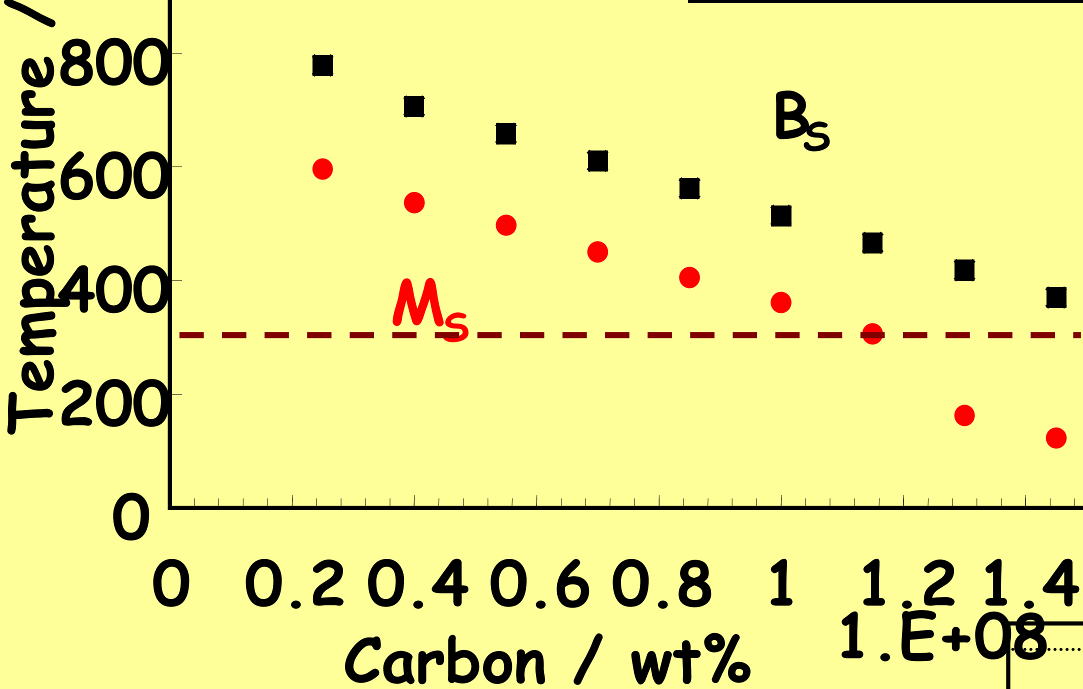

Fe-2Si-3Mn-C wt%

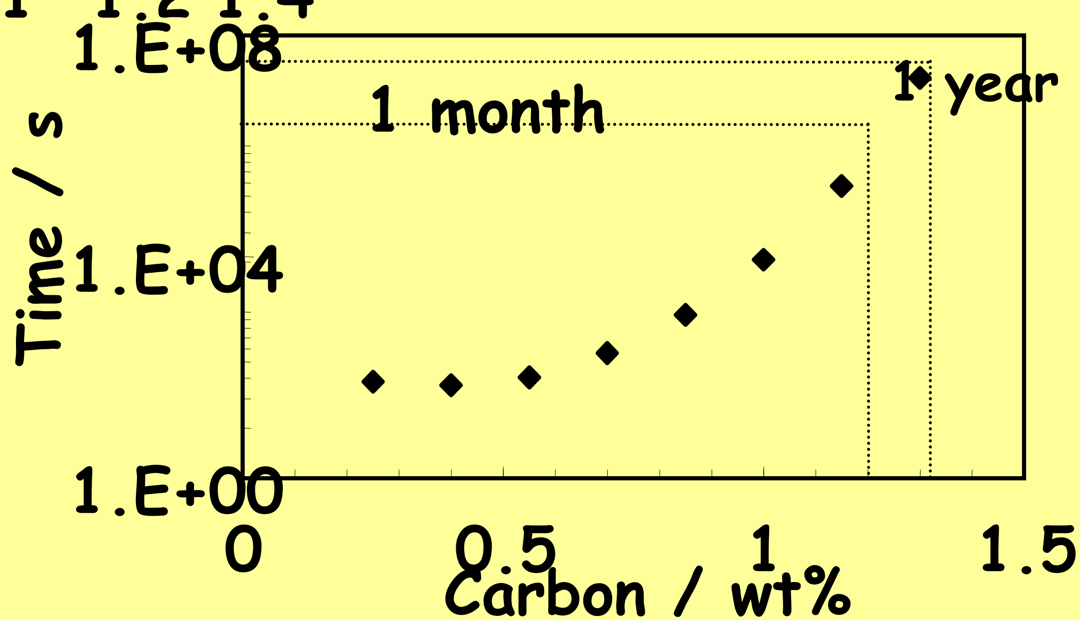

Low transformation temperature

Bainitic hardenability

Reasonable transformation time

Elimination of cementite

Austenite grain size control

Avoidance of temper embrittlement

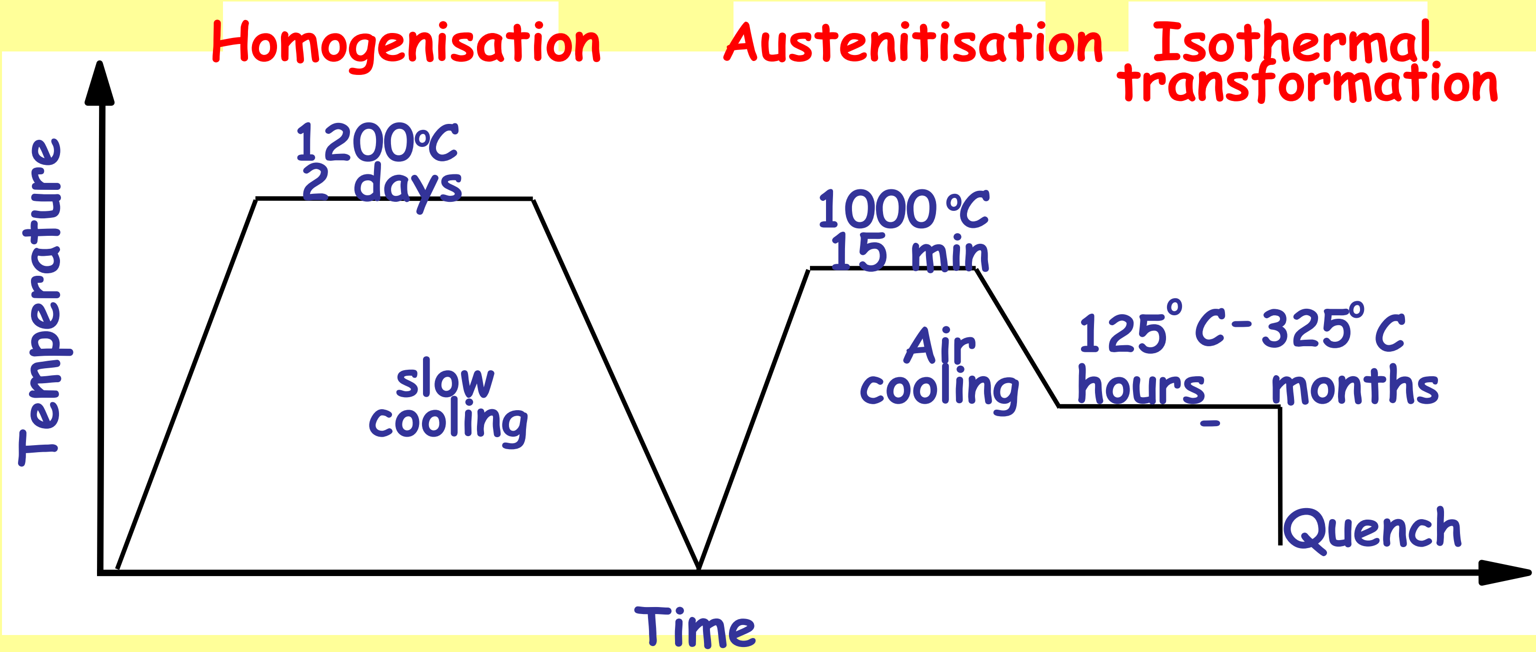

Homogenisation
Austenitisation
Isothermal transformation
Temperature
1200°C
2 days
slow cooling
1000 °C
15 min
Air cooling
125° C - 325° C
hours - months
Quench
Time

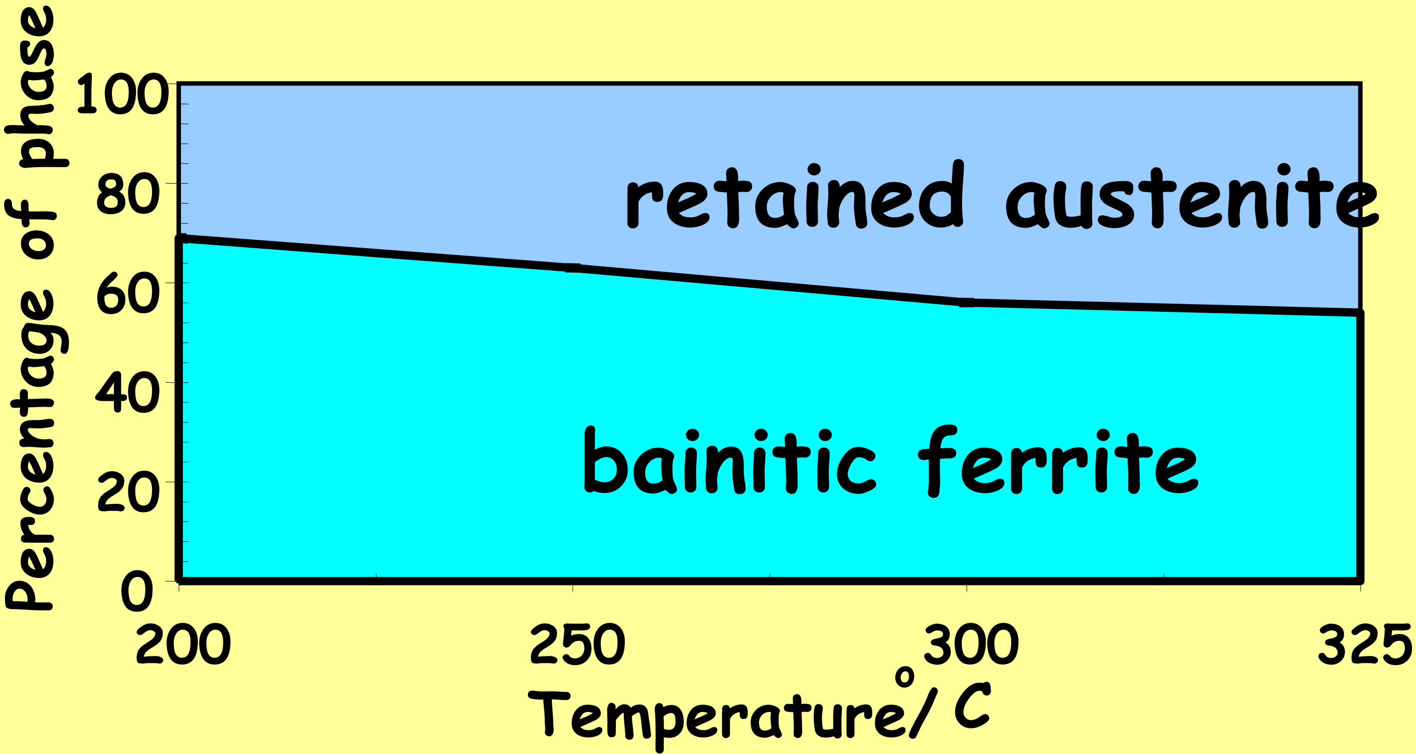

Percentage of phase
100
80
60
40
20
0
retained austenite
bainitic ferrite
200
250
300
325
Temperature/ °C

ballistic mass efficiency

consider unit area of armour

$$BME = \frac{\text{mass of ordinary armour to defeat given threat}}{\text{mass of test material to defeat same threat}}$$

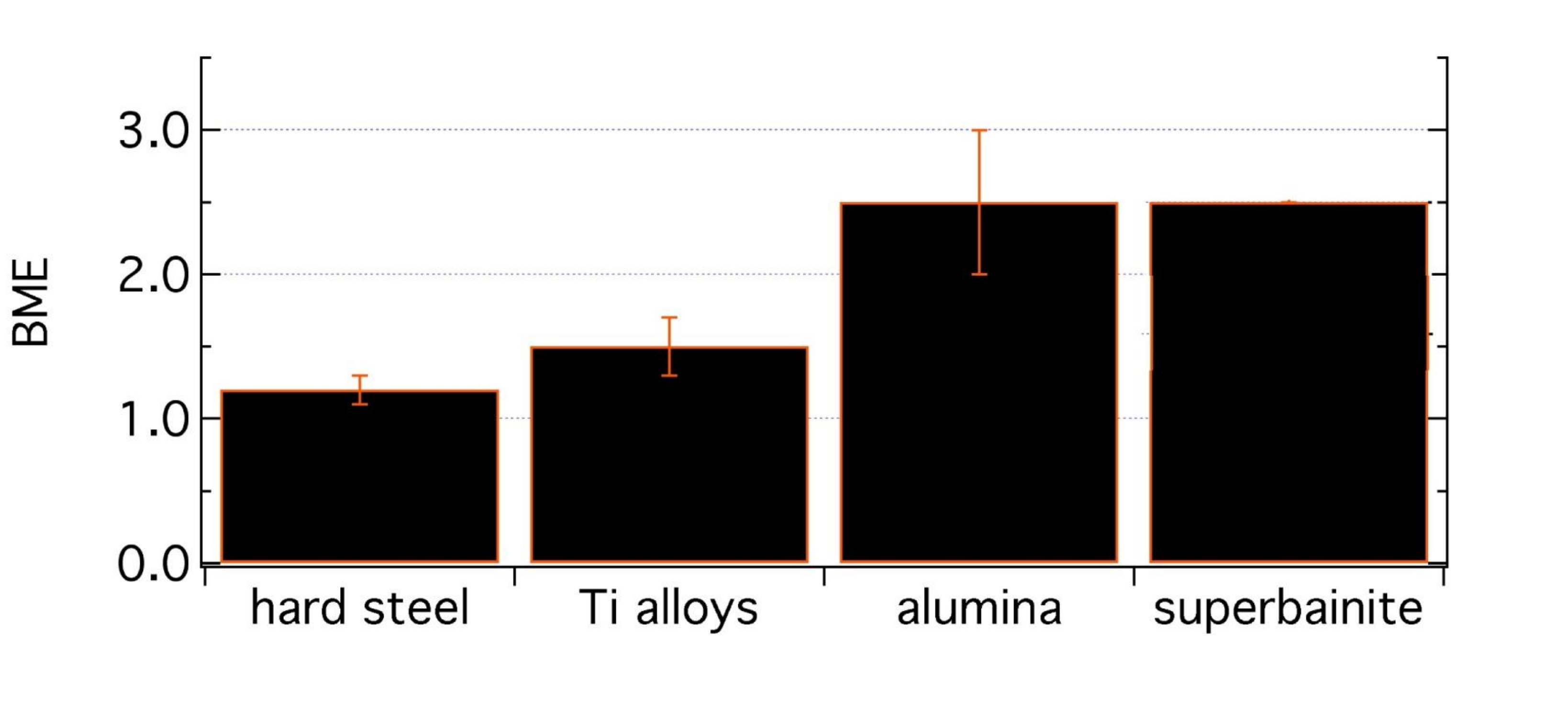


AICHELIN

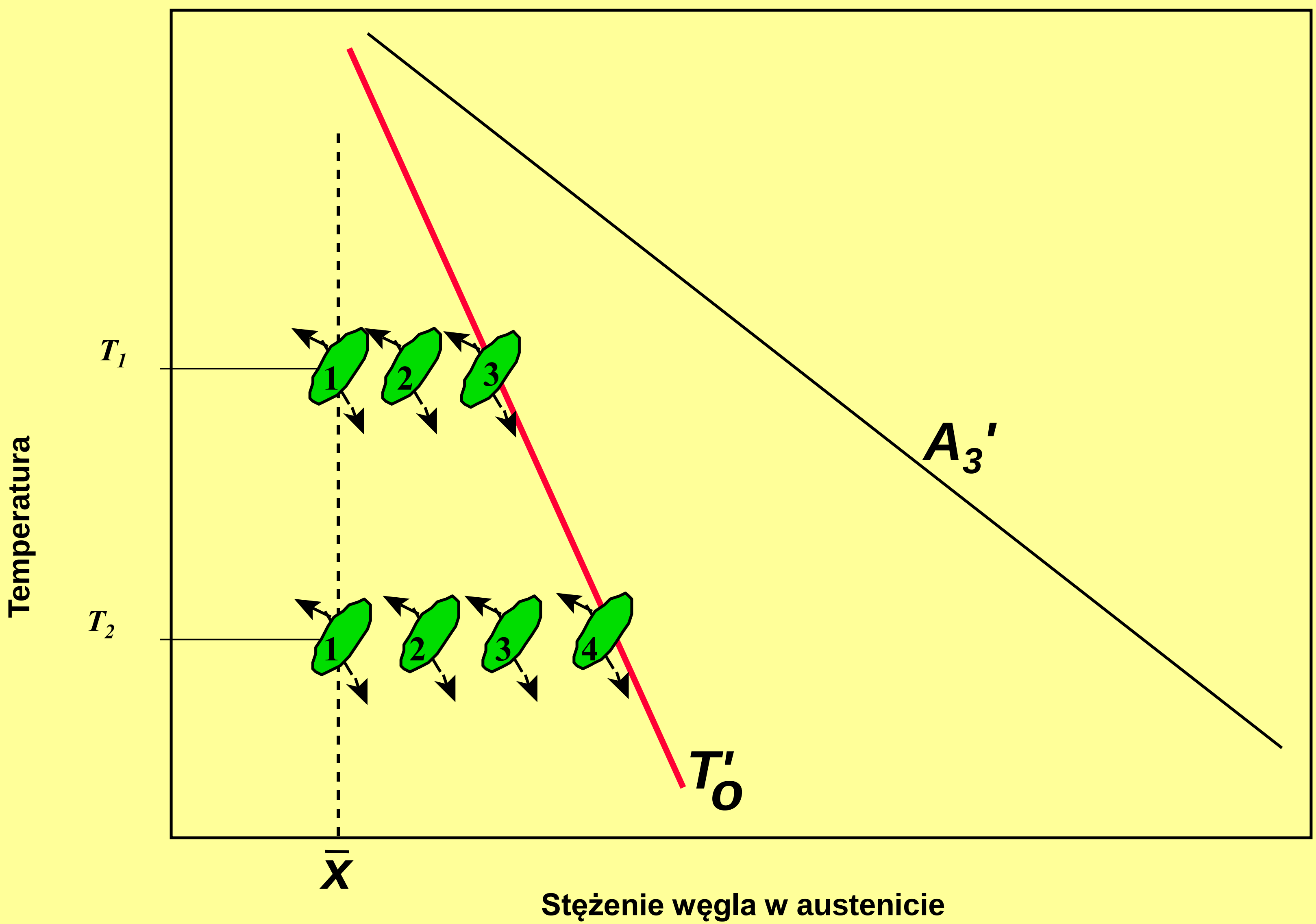

Temperatura
T_1
T_2
1
2
3
1
2
3
4
A_3'
T_0'
$\bar{x}$
Stężenie węgla w austenicie

Bainit low-temperature

Chemical composition in % wt						
Steels	C	Si	Mn	Cr	Mo	V
A	0,79	1,59	1,94	1,33	0,30	0,10
B	0,98	1,46	1,89	1,26	0,26	0,09

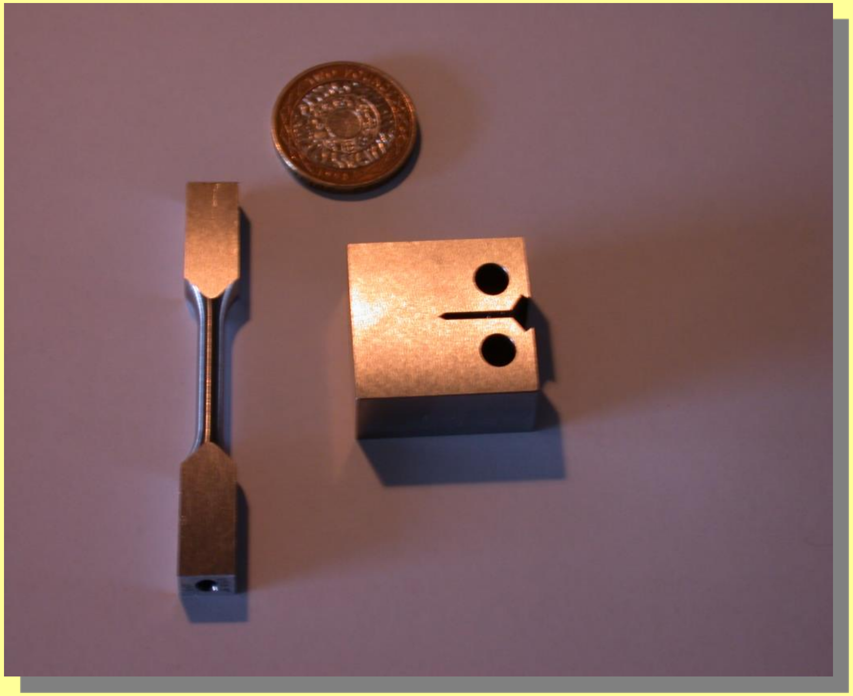

Stal A. Przemiana w 200 ºC:

HV ~ 650 **$R_{0,2}$ ~ 2000 MPa** **R_m ~ 2500 MPa**

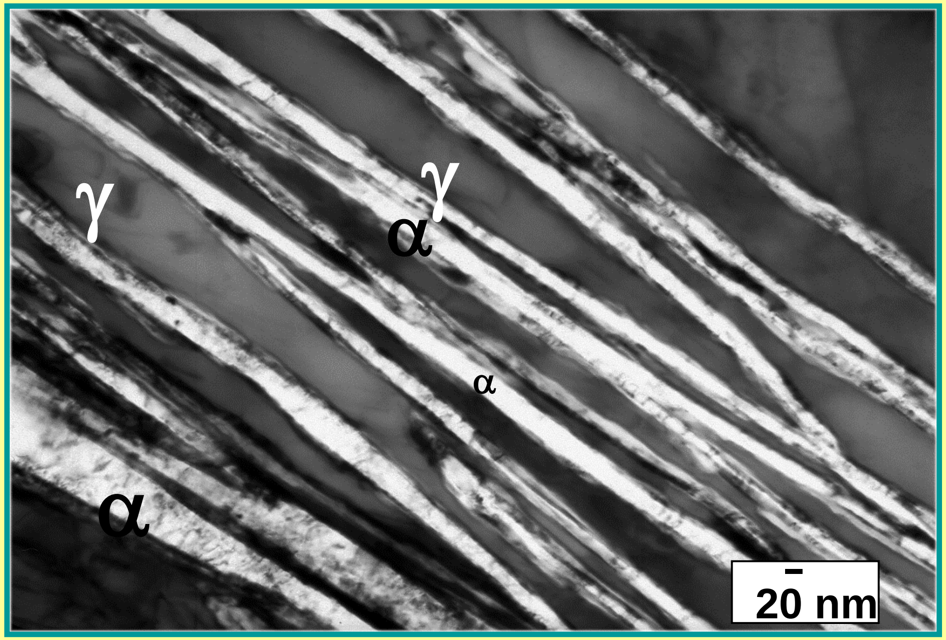

Steel B. transformation at 200 ºC

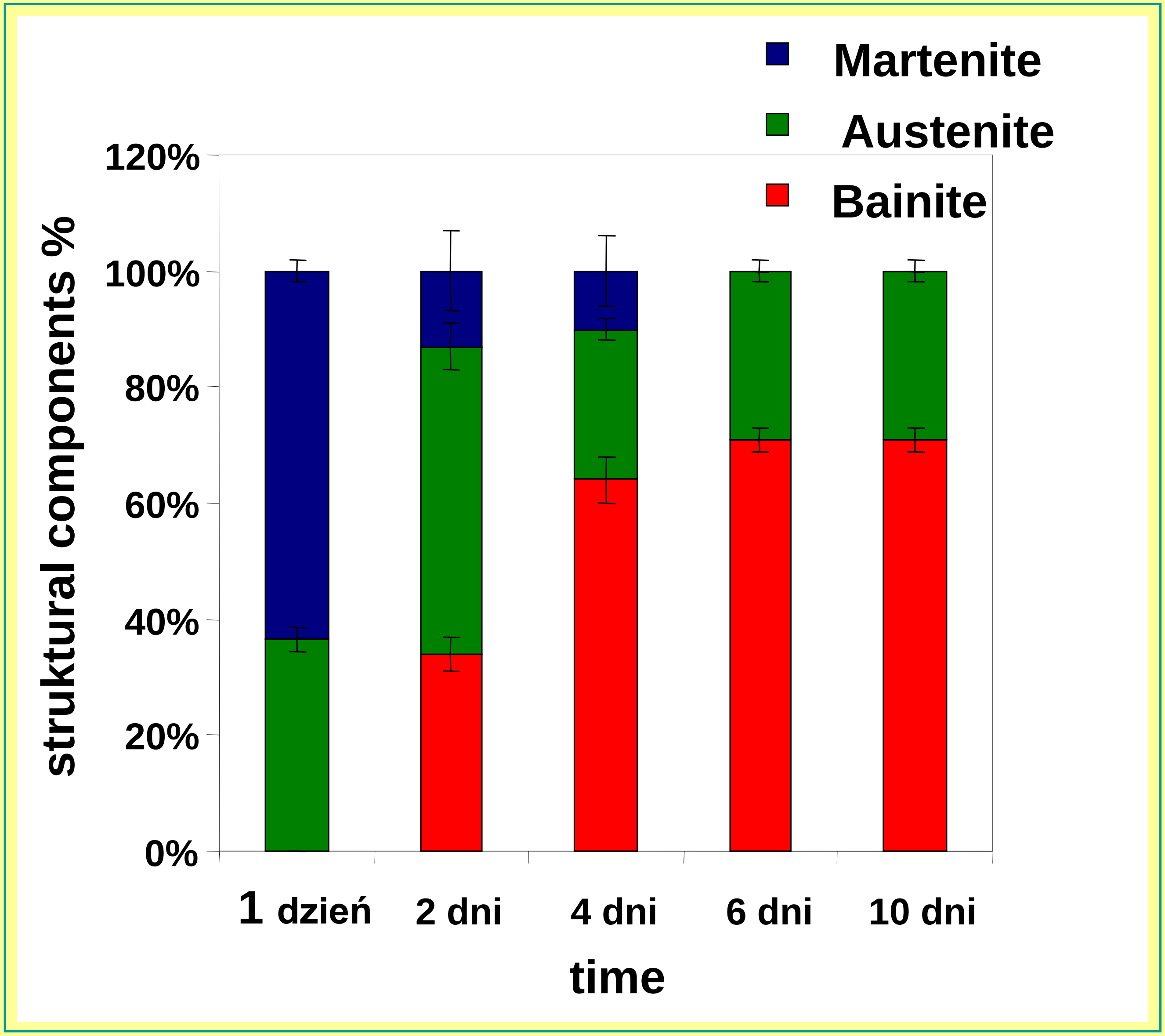

Bainite in rail steels

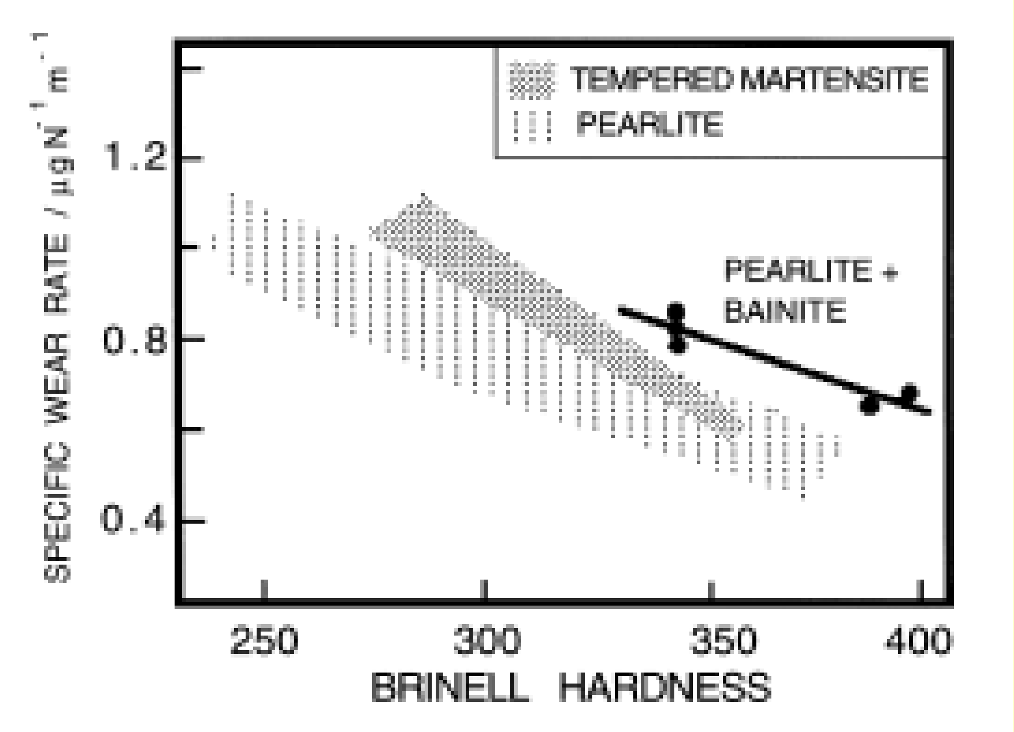

The effect of hardness on the wear of pearlitic bainitic and martensitic steels

Bainite in rail steels